33rd Annual International Conference of the IEEE EMBS
Boston, Massachusetts USA, August 30 - September 3, 2011

Adapting magnetic resonance imaging performance using nonlinear encoding fields

Kelvin J. Layton, Mark Morelande, Peter M. Farrell, Bill Moran, Leigh A. Johnston

***Abstract*— Nonlinear spatial encoding fields for magnetic resonance imaging (MRI) hold great promise to improve on the linear gradient approaches. Unlike the linear techniques, the nonlinear encoding leads to a spatially varying signal-to-noise ratio (SNR). This paper demonstrates the possibility to tailor the encoding fields to focus the high SNR areas to a region of interest. To achieve this, a metric is derived to quantify the spatially dependent performance for arbitrary encoding schemes.**

I. INTRODUCTION

The desire to minimise acquisition time in an magnetic resonance imaging (MRI) experiment has led to the continued introduction of novel imaging schemes from echo planar imaging to parallel imaging [1]. These schemes use linear gradient fields for spatial encoding and usually the fields are setup to acquire samples of the object in the Fourier domain. This supports an intuition regarding the relationship between sampling parameters and image properties such as SNR and resolution. More recently, nonlinear magnetic encoding fields have been investigated and hold great promise to reduce the imaging time of current linear gradient approaches. Such schemes include PatLoc [2] and O-Space imaging [3].

In principle, analysis of the linear reconstruction employed by these schemes is straightforward and the pixel covariance matrix is easily defined. The difficulty lies in computing this covariance for the large matrices associated with practical image resolutions. Fourier imaging and its variations possess a structure that can be exploited to simplify the computation. However, the computation is intractable for arbitrary encoding schemes justifying the development of an approximate metric.

In this paper, we present an analysis of arbitrary encoding schemes by considering frames in the object space. See [4], [5] for an introduction to frame theory. We apply this theory to derive a computationally efficient performance metric for nonlinear encoding schemes.

The reconstruction error in MRI is spatially varying due to a number of factors such as coil sensitivities, irregular sampling and nonlinear encoding fields. Our metric quantifies the spatially varying error for schemes that employ arbitrary nonlinear encoding fields. We demonstrate the utility of the metric by considering a tailored O-Space acquisition to target a region of interest.

The paper is organised as follows. In Section II we review frame theory and apply it to MR imaging. In Section III we derive a performance metric based on the variance of the reconstructed pixels. Finally, in Section IV we demonstrate the usefulness of this metric by considering simulation examples of O-Space imaging.

II. MRI RECONSTRUCTION USING FRAME THEORY

A typical MRI sequence involves the collection of a time series of observations during the formation of a magnetisation echo. This process is repeated for different encoding fields to obtain different projections of the object. Additionally, multiple receiver coils are often used, each with its own spatially varying sensitivity to further encode the object information. We denote the sensitivity function of the l^{th} coil as $c_l(\cdot)$. The measurements for all coils, echoes and time samples are obtained from the signal equation,

$$y_{l,q,i} = \int \rho(\boldsymbol{x}) c_l(\boldsymbol{x}) e^{-j\phi_{q,i}(\boldsymbol{x})} d\boldsymbol{x}. \tag{1}$$

In (1), $\phi_{q,i}(\cdot)$ is the accumulated phase for the q^{th} echo and i^{th} time point, which is critical for spatial encoding of the unknown magnetisation, $\rho(\cdot)$. The phase can be calculated as

$$\phi_{q,i}(\boldsymbol{x}) = \gamma \int_0^{t_i} b_q(\boldsymbol{x}, \tau) d\tau, \tag{2}$$

where γ is the gyromagnetic ratio, $b_q(\boldsymbol{x}, t)$ is the encoding magnetic field, and $t = 0$ denotes the time the excitation pulse is applied. The reconstruction problem is to estimate the object, $\rho(\cdot)$, from a sequence of projections $\{y_{l,q,i}\}$.

We can view these projections as inner products on the space of functions,

$$y_{l,q,i} = \langle \rho, \beta_{l,q,i} \rangle, \tag{3}$$

where we have an index for each coil, l, echo, q, and time, i. The encoding functions, $\beta_{l,q,i}$, are given by

$$\beta_{l,q,i}(\boldsymbol{x}) = c_l(\boldsymbol{x}) e^{j\phi_{q,i}(\boldsymbol{x})}. \tag{4}$$

From this perspective, the reconstruction problem lends itself to a frame theoretic formulation. Frame theory provides results concerning the optimal reconstruction of a function given a sequence of projections, exactly the situation we have in MRI.

A. Matrix Formulation of Frame Theory

We begin with the definition of a frame followed by a matrix formulation that is applicable to MRI reconstruction. For a more rigourous introduction to frame theory consult e.g. [4].

A sequence of functions, $\{\Phi_i\}_{i \in \mathcal{I}}$, in a Hilbert space $\mathcal{V}$, defined over a countable set, $\mathcal{I}$, is a frame if there exists constants, $0 < A \le B < \infty$ such that for all $f \in \mathcal{V}$,

$$A\|f\|^2 \le \sum_{i \in \mathcal{I}} |\langle f, \Phi_i \rangle|^2 \le B\|f\|^2 \tag{5}$$

978-1-4244-4122-8/11/$26.00

where A and B are the lower and upper frame bounds, respectively. We refer to the functions $\{\Phi_i\}_{i\in\mathcal{I}}$ as frame elements. The frame bounds reflect the robustness of the frame elements to perturbations. In the context of MRI, f is the unknown magnetisation and $\mathcal{V}$ is the space of allowable magnetisation functions. It is useful for our application to consider frame elements $\Phi_{l,q,i}$ indexed by coil, echo, and time sample. The definition is readily applicable by considering indices from the set of tuples, $\mathcal{I} = \{(l,q,i) \in [1,\ldots,N_l] \times [1,\ldots,N_q] \times [1,\ldots,N_i]\}$.

When the condition in (5) is satisfied, reconstruction is achieved using the dual frame [4]. In practice we only have a finite number of frame elements so reconstruction of an arbitrary continuous function is impossible. Consequently, we are forced to restrict the space of functions via discretisation. For this purpose we select a pixel basis, $\{\chi_n(\boldsymbol{x})\}_{n=1}^N$, so the object can be represented by a linear combination of the functions, $\chi_n(\boldsymbol{x})$. For example, images can be represented using a rectangular basis where $\chi_n(\boldsymbol{x}) = \mathrm{rect}_W(\boldsymbol{x} - \boldsymbol{x}_n)$. Mathematically, the basis defines a subspace, $\mathcal{U}$, representing the space of allowable functions,

$$\mathcal{U} = \left\{ f \in \mathcal{V} : f(\boldsymbol{x}) = \sum_{n=1}^{N} f_n \chi_n(\boldsymbol{x}) \right\}. \tag{6}$$

In this space, the problem of reconstructing an arbitrary object is transformed to the problem of estimating a set of coefficients, $\{f_n\}$.

Measurements (or frame coefficients) of an unknown function are obtained via the analysis operator, $T : \mathcal{V} \to \mathbb{C}^M$, where M is the number of frame elements. The analysis operator restricted to $\mathcal{U}$ is a map from $\mathbb{C}^N$ to $\mathbb{C}^M$ thus it admits a matrix representation, with elements given by

$$T_{(l,q,i),n} = \langle \chi_n, \Phi_{l,q,i} \rangle. \tag{7}$$

The synthesis operator in this subspace is $T^* : \mathbb{C}^M \to \mathcal{U}$,

$$T^*_{n,(l,q,i)} = \langle \Phi_{l,q,i}, \chi_n \rangle. \tag{8}$$

which can be represented as T', where T' is the conjugate transpose of T defined in (7).

Finally, we define the frame operator, $Q : \mathcal{U} \to \mathcal{U}$ as the composition of the synthesis and analysis operators. In matrix notation,

$$Q = T'T \tag{9}$$

The reconstruction operator using the dual frame [4] simplifies to the Moore-Penrose pseudoinverse,

$$F = Q^{-1}T' = (T'T)^{-1}T'. \tag{10}$$

When we select the frame elements to be the encoding functions used in MRI, $\Phi_{l,q,i} = \beta_{l,q,i}$, and choose a pixel basis, $\{\chi_n\}_{n=1}^N$, the analysis matrix in (7) becomes the standard encoding matrix used in MRI literature [6],

$$E_{(l,q,i),n} = \langle \chi_n, \beta_{l,q,i} \rangle \tag{11}$$

In this case, the measurements $\{y_{l,q,i}\}$ correspond to the frame coefficients. In practice, the Dirac delta distribution is often chosen as the pixel basis since it greatly simplifies the computation of the encoding matrix.

III. Performance Metrics

The impact of noise in the measurements must be considered for practical applications of the above theory. Reconstruction of noisy projections using the dual frame was shown to give the minimum mean square error (MMSE) estimate, with global performance given by the frame bounds [5]. For nonlinear encoding fields, the error is spatially varying and a local performance metric is required. Although the variance of each reconstructed pixel is a natural performance metric, the computation is intractable for realistic resolutions and thus we derive an appropriate approximation.

A. Reconstruction Variance

The signal model in (3) is modified to include additive noise,

$$y_{l,q,i} = \langle \rho, \beta_{l,q,i} \rangle + w_{l,q,i}. \tag{12}$$

A discretised object can be represented by the vector, $\boldsymbol{f} = [f_1,\ldots,f_N]^T$, where the elements are, $f_n = \langle \chi_n, \rho \rangle$. We construct the vectors, $\boldsymbol{y} = [y_{1,1,1},\ldots,y_{N_l,N_q,N_i}]^T$ and $\boldsymbol{w} = [w_{1,1,1},\ldots,w_{N_l,N_q,N_i}]^T$ so (12) can be written as the matrix equation,

$$\boldsymbol{y} = E\boldsymbol{f} + \boldsymbol{w}, \tag{13}$$

with $\boldsymbol{w} \sim \mathcal{N}(0,\Sigma)$ for a general covariance matrix Σ.

We desire a frame operator that adequately models the covariance so we consider the general case where the frame elements are a linear combination of encoding functions,

$$\Phi_{l,q,i} = \sum_{l',q',i'} \Gamma_{(l,q,i),(l',q',i')} \beta_{l',q',i'}. \tag{14}$$

This leads to frame coefficients that are a linear combination of the MRI measurements. Let Γ be a matrix of weights with elements $\Gamma_{(l,q,i),(l',q',i')}$; the coefficients can be defined by the matrix equation, $\boldsymbol{g} = \Gamma\boldsymbol{y}$, with $\boldsymbol{g} \sim \mathcal{N}(\Gamma E\boldsymbol{f}, \Gamma\Sigma\Gamma')$.

The analysis operator is $T = \Gamma E$ and recall the frame matrix is $Q = T'T$. The reconstructed coefficients are given by $\hat{\boldsymbol{f}} = F\boldsymbol{g}$, where F is the reconstruction operator in (10). The covariance of the reconstructed coefficients is

$$X = (T'T)^{-1}T'\Gamma\Sigma\Gamma'T'(T'T)^{-1} \tag{15}$$

The definition of Σ allows the following decomposition, $\Sigma^{-1} = \Sigma^{-1/2}\Sigma^{-1/2}$. The main result of this section is that selecting the set of weights to be

$$\Gamma_{(l,q,i),(l',q',i')} = [\Sigma^{-1/2}]_{(l,q,i),(l',q',i')} \tag{16}$$

yields a covariance of

$$X = Q^{-1}. \tag{17}$$

This equation reveals the close link between the frame elements, frame operator, and the resulting covariance. Importantly, the relationship is valid irrespective of the measurement noise properties, by the appropriate selection of the weighting matrix.

When the condition in (16) is satisfied, the frame matrix can be written in terms of the discretised encoding functions as $Q = E'\Sigma^{-1}E$ or in terms of matrix elements,

$$Q_{n,m} = \sum_{l,q,i} \sum_{l',q',i'} \langle \beta_{l,q,i}, \chi_n \rangle \Sigma^{-1}_{(l,q,i),(l',q',i')} \langle \chi_m, \beta_{l',q',i'} \rangle. \tag{18}$$

This process of transforming the measurements has very close ties to 'noise whitening' in linear estimation theory [7]. This is required in Section IV to analyse a parallel imaging scheme, where noise is correlated between receiver channels [6].

B. Approximate Reconstruction Variance

The pixel variance is obtained by extracting the diagonal elements of the covariance matrix in (17). This is not a suitable metric since the inverse is not feasible to compute for practical matrix sizes. We require an alternative performance metric that: 1) reflects the variance of each reconstructed pixel, 2) is valid for arbitrary encoding fields, and 3) is computationally efficient. In previous work, we defined a simple metric related to the width of the point spread function, extracted from the frame matrix [8]. In this paper, we use a series expansion to define a second-order approximation to the variance.

To this end we exploit the fact that, for most practical imaging schemes, the frame matrix is approximately diagonal. For example, in standard Fourier imaging the matrix is exactly diagonal and the only distortion is due to the truncation effects associated with the projection operator. The approximate diagonal nature of the frame matrix, Q, suggests a decomposition of the matrix into its diagonal part, Λ, and off-diagonal part, Z, such that $Z = Q - \Lambda$. We take the Taylor series of Q^{-1} about $Q = \Lambda$ to get the m^{th} order approximation,

$$Q_m^{-1} = \sum_{n=0}^{m} (-\Lambda^{-1}Z)^n \Lambda^{-1}. \tag{19}$$

The series will converge when $\|\Lambda^{-1}Z\| < 1$, where $\|\cdot\|$ denotes the subordinate matrix norm. By definition, Λ is diagonal so Λ^{-1} is easily computed, which leads to approximations that can be efficiently computed. If we consider the diagonal elements of the first order approximation, Q_1^{-1}, we notice that $\operatorname{diag}(\Lambda^{-1}Z\Lambda^{-1}) = \mathbf{0}$, so we need to use the second order approximation for useful results.

The computation is further reduced since the diagonal components can be calculated individually as follows. Let $z_{n,p}$ denote the elements of Z and let the diagonal elements of Λ^{-1} be $\alpha_n, n = 1, \ldots, N$. The diagonal elements of Q_2^{-1} are

$$[Q_2^{-1}]_{pp} = \alpha_p \left(1 + \alpha_p \sum_{n=1}^{N} z_{n,p}^2 \alpha_n \right) \tag{20}$$

which can be calculated row by row, without the need to calculate or store the large matrix, Q.

The metric defined by (20) satisfies all of our requirements. It is relatively easy to compute, applicable to general encoding schemes and reflects the variance of individual pixels. In Section IV we use our metric to produce a map of the spatially varying performance of different imaging configurations.

IV. Simulation Example

The metric developed in this paper is demonstrated by considering the problem of tailoring an acquisition to focus on a region-of-interest. To elaborate suppose we are interested in imaging the right side of the cerebral cortex; we don't care about the image quality on the left side. In this section, we prove that it is possible to tune the nonlinear encoding fields to obtain improved imaging performance in the desired region. Our metric allows us to determine the performance across the image *a priori*, necessary for experimental design. We examine this problem in the context of the recently developed O-Space imaging [3].

A. O-Space Imaging

O-Space imaging is a technique that uses nonlinear encoding fields and boasts rapid imaging times [3]. The technique consists of a quadratic encoding field that is translated after every echo. The field is given by $b_q(\boldsymbol{x}, t) = b_q(\boldsymbol{x}) = G\|\boldsymbol{x} - \boldsymbol{r}_q\|^2$ so the phase functions defined in (2) are $\phi_{q,i}(\boldsymbol{x}) = \gamma G \|\boldsymbol{x} - \boldsymbol{r}_q\|^2 t_i$ and the encoding functions in (4) become

$$\beta_{l,q,i}(\boldsymbol{x}) = c_l(\boldsymbol{x}) e^{j\gamma G \|\boldsymbol{x} - \boldsymbol{r}_q\|^2 t_i}. \tag{21}$$

The field centre points, $\{\boldsymbol{r}_q\}$, can be selected to focus the imaging on a region of interest. The complicated structure of this encoding precludes a performance analysis similar to that of the PatLoc technique [9]. The frame-oriented approach developed in this paper is readily applicable.

We proceed following the theory developed in Section III. The noise in a parallel MRI experiment is correlated between channels, not between echoes or time samples, thus $\Sigma^{-1}_{(l,q,i),(l',q',i')} = \delta_{q,q'}\delta_{i,i'}\Sigma^{-1}_{l,l'}$. We impose the noise whitening condition in (16) and adopt the ideal pixel basis of delta functions, $\chi_i(\boldsymbol{x}) = \delta(\boldsymbol{x} - \boldsymbol{x}_i)$. The frame matrix elements are computed using (18) as

$$Q_{n,m} = \kappa(\boldsymbol{x}_n, \boldsymbol{x}_m) \sum_{q,i} e^{j\gamma(b_q(\boldsymbol{x}_n) - b_q(\boldsymbol{x}_m))t_i} \tag{22}$$

where κ is the noise-adjusted coil kernel given by

$$\kappa(\boldsymbol{x}_n, \boldsymbol{x}_m) = \sum_{l,l'} c_l(\boldsymbol{x}_n) \Sigma^{-1}_{l,l'} c_{l'}(\boldsymbol{x}_m). \tag{23}$$

This coil kernel arises from the use of multiple receiver coils with spatially varying sensitivities.

We now use the metric in (20) to quantify the spatially varying performance for different centre point configurations.

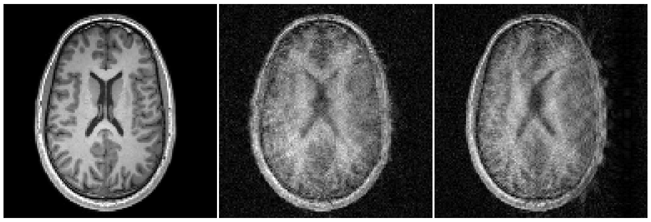

(a) (b) (c)

Fig. 2: The numerical phantom (a) used for simulations, obtained from a T_2 weighted image of a human brain. The reconstructed images (b,c) from the centre point configurations in Fig. 1(a,b), respectively.

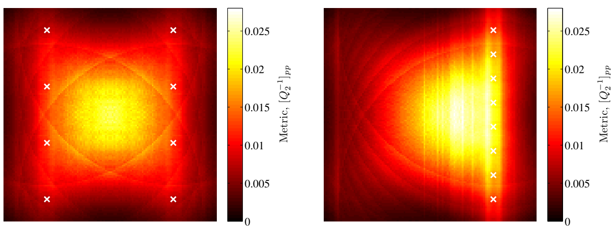

(a) (b)

Fig. 1: The proposed metric for different centre point configurations of an O-Space imaging scheme. The centre points are marked with white $\times$'s.

B. Tailored Acquisition

O-Space imaging acquisitions are simulated with parameters comparable to the original implementation in [3]. Eight receive coils are placed concentrically around the field-of-view with sensitivities simulated by the magnetostatic limit of the Biot-Savart equation. Eight echoes are collected representing a high undersampling of $R = 16$. We consider two different centre point configurations. The first acquisition has centre points arranged evenly on both sides of the field of view. The second acquisition has centre points arranged on the left side of the field-of-view. In both cases, the final image resolution is 128×128 and the number of readout samples is $N_i = 256$.

For this setup it is cumbersome to perform the matrix inversion and the advantage of our metric is apparent. The metric is calculated for both centre point configurations to demonstrate the spatially varying performance. Fig. 1 displays the variance maps for each centre point configuration. The centre points are marked on the corresponding maps with white $\times$'s. When the centre points are located to the right side of the field-of-view, the variance on the left side is decreased. This is intuitive since the quadratic encoding improves with increasing distance from the centre points. The metric quantifies this effect and allows us to design a configuration that leads to decreased noise in the region of interest.

The data sets are obtained through simulating the acquisition of a numerical brain phantom in Fig. 2(a). Complex Gaussian noise is added to the measurements with a standard deviation equal to 5% of the mean phantom intensity. We reconstruct the images by solving the large matrix equation using a conjugate gradient algorithm similar to [6].

Fig. 2(b,c) contain the reconstructed images for the centre point configurations shown in Fig. 1(a,b), respectively. To quantify the reconstruction error in the region of interest, the mean squared error (MSE) of the pixels located on the left side of the image is calculated. The MSE in this region is 0.0103 and 0.0082 for Fig. 2(b,c), respectively. Fig. 2(c) corresponds to right-sided centre points and exhibits smaller error on the left side of the image, particularly near the skull. Conversely, the evenly distributed centre points result in an image with more uniform error, illustrated in Fig. 2(b).

V. Conclusion

We apply the theory of frames to MRI schemes that employ nonlinear spatial encoding magnetic fields. This theory allows the derivation of a computationally efficient and intuitive performance metric. The metric is a second order approximation to the variance of the reconstructed pixels and can be applied to arbitrary encoding schemes. We calculate our metric for O-Space imaging examples to demonstrate the spatially varying performance. In this way, we can devise acquisition schemes that provide superior performance in a given region of interest.

References

[1] E. Haacke, R. Brown, M. Thompson, and R. Venkatesan, *Magnetic resonance imaging: Physical principles and sequence design*. John Wiley and Sons, 1999.

[2] J. Hennig, A. Welz, G. Schultz, J. Korvink, Z. Liu, O. Speck, and M. Zaitsev, "Parallel imaging in non-bijective, curvilinear magnetic field gradients: A concept study," *Magnetic Resonance Materials in Physics, Biology and Medicine*, vol. 21, no. 1-2, pp. 5–14, 2008.

[3] J. Stockmann, P. Ciris, G. Galiana, L. Tam, and R. Constable, "O-space imaging: Highly efficient parallel imaging using second-order nonlinear fields as encoding gradients with no phase encoding," *Magnetic Resonance in Medicine*, vol. 64, no. 2, pp. 447–456, 2010.

[4] O. Christensen, *Frames and Bases: An Introductory Course*. Birkhäuser, 2008.

[5] S. Mallat, *A wavelet tour of signal processing*. Academic Press, 1999.

[6] K. Pruessmann, M. Weiger, P. Börnert, and P. Boesiger, "Advances in sensitivity encoding with arbitrary k-space trajectories," *Magnetic Resonance in Medicine*, vol. 46, no. 4, pp. 638–651, 2001.

[7] S. Kay, *Fundamentals of Statistical Signal Processing: Estimation Theory*. Prentice-Hall, 1993.

[8] K. Layton, M. Morelande, P. Farrell, B. Moran, and L. Johnston, "A performance measure for MRI with nonlinear encoding fields," in *Proceedings of the ISMRM 19th Annual Meeting*, 2011.

[9] G. Schultz, P. Ullmann, H. Lehr, A. Welz, J. Hennig, and M. Zaitsev, "Reconstruction of MRI data encoded with arbitrarily shaped, curvilinear, nonbijective magnetic fields," *Magnetic Resonance in Medicine*, vol. 64, no. 5, pp. 1390–1403, 2010.